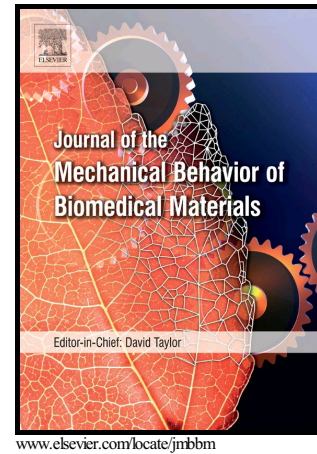


Author's Accepted Manuscript

Interaction of ACP and MDP and its effect on dentin bonding performance

Ling Zhang, Wenting Wang, Chaoyang Wang, Mingxing Li, Zhe Wang, Zhiwei Su, Baiping Fu



PII: S1751-6161(18)31216-5
DOI: <https://doi.org/10.1016/j.jmbbm.2018.12.017>
Reference: JMBBM3102

To appear in: *Journal of the Mechanical Behavior of Biomedical Materials*

Received date: 21 August 2018
Revised date: 14 December 2018
Accepted date: 16 December 2018

Cite this article as: Ling Zhang, Wenting Wang, Chaoyang Wang, Mingxing Li, Zhe Wang, Zhiwei Su and Baiping Fu, Interaction of ACP and MDP and its effect on dentin bonding performance, *Journal of the Mechanical Behavior of Biomedical Materials*, <https://doi.org/10.1016/j.jmbbm.2018.12.017>

This is a PDF file of an unedited manuscript that has been accepted for publication. As a service to our customers we are providing this early version of the manuscript. The manuscript will undergo copyediting, typesetting, and review of the resulting galley proof before it is published in its final citable form. Please note that during the production process errors may be discovered which could affect the content, and all legal disclaimers that apply to the journal pertain.

Interaction of ACP and MDP and its effect on dentin bonding performance

Ling Zhang,^{a,b}, Wenting Wang,^{a,b}, Chaoyang Wang^{a,b}, Mingxing Li^{a,b}, Zhe Wang^{a,b}, Zhiwei Su^{a,b}, Baiping Fu^{a,b,1*}

^a Department of Prosthodontics, Hospital of Stomatology Affiliated to Zhejiang University School of Medicine, Yan'an Road 395, Hangzhou 310006, Zhejiang, China

^b Key Laboratory for Oral Biomedical Research of Zhejiang Province, Hangzhou 310006, Zhejiang, China

fbp@zju.edu.cn

Abstract**Objectives:**

The study investigated the solid reactants of amorphous calcium phosphate (ACP) nanoparticles with 10-methacryloyloxydecyl dihydrogen phosphate (MDP) in ethanol-aqueous solution, and the effect of ACP-MDP suspension as a novel primer on dentin micro-tensile bond strengths (MTBS) prior to application of self-etch adhesives.

Materials and Methods:

The ACP nanoparticles were synthesized. The solid reactants of ACP nanoparticles with MDP ethanol-aqueous solution were analyzed by TEM, SEM, XRD and AFM. After the ACP-MDP complexes were attacked by alkaline, acidic and self-etch adhesive challenges, they were analyzed with TEM. The polished mid-coronal dentin surfaces of six third molars were treated with ACP-MDP suspension, 5% MDP solution or not (served as control), and thoroughly water-sprayed. The pretreated dentin surfaces were applied with a self-etch adhesive (Clearfil S3 Bond) and placed with a composite resin (Clearfil Majesty). After 24 hrs,

¹ Tel/Fax: +86-571-87217427

the resin-bonded samples were cut into multiple beams before the MTBS tests were performed. The failure modes were determined by a stereo-microscopy. The pretreated dentin surfaces were analyzed by SEM. The resin-dentin interfaces were analyzed with TEM.

Results:

The ACP nanoparticles in the MDP ethanol-aqueous solution at certain molar ratio of Ca:MDP (0.12:1) could self-assemble into ACP-MDP complexes consisting of nanolayering structures. The ACP-MDP self-assembly went from ACP nanoparticles, beaded structures, and twig-like structures to networks. The ACP-MDP complexes can be resistant to adhesive challenge, but not to alkaline and acidic challenges. ACP-MDP complexes possessed a similar modulus of elasticity to dentin, and were stable at least for 3 months. Furthermore, the dentin surfaces treated with ACP-MDP suspension could significantly increase the dentin MTBS when compared with control and those treated with 5% MDP solution ($P < 0.05$).

Conclusion:

The ACP-MDP suspension at certain molar ratio of Ca:MDP (0.12:1) could be self-assembled into ACP-MDP complexes consisting of nanolayering structures, and could be used as a novel primer to greatly improve the dentin bond strengths.

Keywords: amorphous calcium phosphate, nano-layering, biomimetic fabrication, dentin bond strengths

1. Introduction

In nature, biomaterials are usually composed of the well-organized organic-inorganic hybrid structures, revealing the unique physicochemical properties, such as bone and tooth (Mann, 2011; Weiner et al., 1998; Busch et al., 2001). The organic molecules are believed to be able to regulate the shape and properties of inorganic crystals (Meldrum et al., 2008). Meanwhile, salt ions play a critical role in the self-assembled structures and their function (Pedersen et al., 2006; Klement et al., 2007; Jain et al., 2010). Scientists take efforts to use the

two distinctly different organic and inorganic phases to design and synthesize the highly-ordered and periodic assembly of organic-inorganic nanostructures. Hence, it is still a great challenge in the laboratory to prefabricate organic-inorganic nanostructures by using a simple bottom-up fabrication from salt ions and organic molecules.

In dental materials engineering, contemporary dentin adhesive systems are reliable and can achieve stable bond durability however technique sensitivity triggers a serious issue for practitioners during clinical application procedures (Manuja et al., 2012; Iovan et al., 2017). Hence, the development of smart materials could promote dentin bonding performance of contemporary dentin adhesives (Liu et al., 2011). According to the previous studies, organic-inorganic hybrid such as nano-layering structure has been proven to improve bond durability (Yoshida et al., 2004; Fukegawa et al., 2006; Yoshihara et al., 2010; Koshiro et al., 2006) and prevent the hybrid layer from biodegradation (Breschi et al., 2008). Recent report demonstrated that the nano-layering structures resulted from interaction of 10-methacryloyloxydecyl dihydrogen phosphate (MDP) with synthetic hydroxyapatite (HAp) powder (Fukegawa et al., 2006; Yoshihara et al., 2010) and enamel/dentin (Yoshihara et al., 2011). The acidic functional organic molecules can interact with calcium species at the organic-inorganic interfaces (Zhai et al., 2010a). The acidic functional monomers of the dental adhesives are considered to be critical to the bond performance of the self-etch adhesives (Van Landuyt et al., 2007). The acidic functional monomer (MDP) has been demonstrated to chemically bond to hydroxyapatite (HAp), forming a periodic nano-layering structure (Fukegawa et al., 2006; Yoshihara et al., 2010; Yoshihara et al., 2011). Calcium phosphate, main component of biological bone and tooth, shows excellent biocompatible properties (Dorozhkin et al., 2002). Nanoparticles of amorphous calcium phosphate (ACP) are the least stable of the calcium phosphate phases (Weiner et al., 2005). In supersaturated solutions, ACP nano-precursors usually transforms into the stable crystalline phase (Wang et al., 2009). They are widely involved in biomimetic mineralizations, including dentin

generation (Mahamid et al., 2008; Combes et al., 2010), since they are used as a nanoprecursor to deliver biomimetic mineralization (Niu et al., 2014).

A challenging question is raised whether a novel primer consisting of inorganic (ACP) and organic (MDP) materials can be prepared via the self-assembly process of organic-inorganic hybrid mesocrystals in laboratory. To understand the physicochemical regulations of the nano-layering structure is critical to materials science since it can enrich our knowledge of biomaterials science using ‘bottom-up’ nanotechnology for functional biomaterials design and fabrication.

The objectives of this study were to investigate 1) the solid reactants of interaction of ACP nanoparticles with MDP in ethano-aqueous solution; 2) and the effect of ACP-MDP suspension on dentin bond strengths prior to application of self-etch adhesives. The null hypotheses tested in this study were that 1) the nano-layering structure could not be self-assembled via a bottom-up way; and 2) pretreatment with ACP-MDP suspension prior to application of self-etch adhesives could not improve the dentin bond effectiveness.

2. Materials and Methods

2.1. Materials

Double distilled water was used in the experiment. The chemicals ($\text{CaCl}_2 \cdot 2\text{H}_2\text{O}$, Na_2HPO_4) were of chemical analytical grade and purchased from Sigma-Aldrich, USA and Aladdin, China, respectively. Their solutions were filtered twice through Millipore films (0.22 μm) prior to use. MDP (Watson International Ltd., Jiangsu, China) were used directly without further purification.

2.2. Characterizations

Scanning electron microscopy (SEM) was performed with a ZEISS ULTRA 55 microscope, Oberkochen, Germany at an acceleration voltage of 5 kV. Transmission electron

microscopy (TEM) was performed with a JEM-1200EX TEM, Tokyo, Japan at an acceleration voltage of 100 kV. The high-resolution TEM (HRTEM) was performed with Philips CM200UT HRTEM, Eindhoven, Holland at an acceleration voltage of 160 kV. Small and wide angle X-ray diffraction (SAXRD, WAXRD) was performed using a Rigaku D/max-2550pc, Tokyo, Japan with monochromatized Cu K α radiation and 0.02° scanning step. The Fourier transform infrared spectroscopy (FTIR) was performed with a Nexus-670 spectrometer, Madison, USA, from 400 to 4000 cm⁻¹ in transmission mode. The quantitative measurement of the mechanical property was performed with an atomic force microscopy (AFM), Veeco Nanoscope IVa, Santa Barbara, CA, USA, using an E head and a silica tip (Veeco, USA) on a cantilever with a spring constant of 7.4 N m⁻¹ at a scanning rate of 60 nm s⁻¹. The cantilever deflection represents a force curve produced by a Veeco multimode scanning probe with Nano IVa controller. The concentrations of Ca ions released from ACP nanoparticles (0.01 g) were measured by inductively coupled plasma-atomic emission spectrometry (ICP-AES), Thermo ICAP-6000, USA.

2.3. Synthesis and characterization of ACP nanoparticles

One hundred μ L of 1M NaOH solution was added into 100 mL of 12 mM Na₂HPO₄ solution at room temperature. Afterward, 100 mL of 20 mM CaCl₂ solution was poured into the solution within 5 s under vigorous stirring. The suspension was centrifuged at 6000 rpm at -5 °C to obtain the precipitates (ACP nanoparticles). They were washed twice with 5 mL of ethanol (EtOH) and dried under vacuum at 40 \pm 1 °C. The ACP nanoparticles were characterized by TEM, SEM and FTIR.

2.4. Interaction of MDP with ACP nanoparticles

The ACP nanoparticles (0.01g) were dispersed in 4 mL of a MDP/EtOH/H₂O (5:48:47 wt%) solution at a temperature of 37°C. After the suspensions were kept for 5 min, 10 min, 20

min, 30 min, 3 hrs, 5 hrs, 1 d, 2 d, 3 d, 4 d, 5 d and 3 months, respectively, they were centrifuged to harvest the precipitates (ACP-MDP complexes). Subsequently, they were further washed twice with absolute ethanol and dried under a vacuum at 40 ± 1 °C before they were characterized with TEM, SEM, HRTEM, SAXRD, WAXRD, and AFM.

The ACP nanoparticles (0.01g) were dispersed in 4 mL of a MDP ethanol-aqueous solution (10% wt, 15% wt or 20% wt) at a temperature of 37°C. After 2 d, the suspension were centrifuged to obtain the solid reactants and the supernatant was discarded. Thereafter, the reactants were rinsed twice with absolute ethanol, and totally dried under a vacuum at 40 ± 1 °C before they were characterized with TEM and XRD. Four mL of ethanol-aqueous (1:1) solution, in which 5% wt of MDP had been dissolved, was each added with 0.02 g, 0.03 g, or 0.05 g of ACP nanoparticles at a temperature of 37°C, respectively. After 2 d, the reactants were respectively prepared as the above-mentioned, and then analyzed with TEM and XRD.

2.5. Stability tests of ACP-MDP Complexes

The aforementioned ACP-MDP complexes (5 wt% MDP + 0.01 g ACP) were immersed into 100 μ L of 0.01 mM HCl (pH \approx 5), 5 wt% NaOCl (pH \approx 13) or the self-etch adhesive Clearfil S3 Bond (pH \approx 2.7) for 15 min. Subsequently, they were further washed twice with double distilled water before they were analyzed with HRTEM.

2.6. Micro-tensile bond strengths (MTBS) tests

2.6.1. Preparation of ACP-MDP suspension

ACP-MDP suspensions (5 wt% MDP + 0.01 g ACP) were prepared as above-mentioned and kept for 2 d before use.

2.6.2. MTBS tests

Six non-carious and defect-free human third molars were stored in 0.5 wt% chloramine T at 4°C and used within 1 month after extraction. The teeth were collected with

the informed consent. The protocol was performed in accordance with the international Ethical Guideline and Declaration of Helsinki (World Medical Association, 2013), and approved by the Institutional Ethic Board (#201603). The mid-coronal dentin surfaces were exposed by cutting off the cusps. After six dentin surfaces were wet-ground with 320-grit SiC abrasive paper and water-sprayed, two of them were not further treated (served as control) and four of them were treated either with 5% MDP ethanol-aqueous solution or with ACP-MDP suspension for 30 s, and water-sprayed for 60 s. Subsequently, a mild self-etch adhesive Clearfil S3 Bond (Kuraray-Noritake Co., Japan) was applied to the pre-treated dentin surfaces for 20 s, gently air-dried for 5 s, and light-cured for 20 s. Subsequently, two 2-mm increments of a composite resin Clearfil Majesty (Kuraray-Noritake Co., Japan) were placed, and light-cured for 40 s, respectively. After 24 hrs of storage in tap water, the specimens were prepared into multiple beams of approximately 1 x 1 x 9 mm through the dentin-resin interface with a low-speed saw (Isomet 1000, Buehler, USA). The specimens were fixed with a cyanoacrylate glue (Zapit DVA; Corona, CA, USA) onto the grips of a microtensile device and the MTBS tests were performed with a Micro Tensile Tester (Bisco, USA) at a cross-head speed of 1 mm/min until fracture. The MTBS was calculated in MPa. The specimens suffered from pre-testing failures during the specimen preparation procedure were excluded in the study.

2.6.3. Failure Modes

After the MTBS tests, the failure modes were determined by a stereo-microscopy (Leica MZAPO, Germany) at 50-fold magnifications, which were categorized into adhesive failure at the dentin-resin interface, cohesive failure within dentin or composite, and mixed failure (Armstrong et al., 2010).

2.6.4. SEM Observations

Another three pieces of polished dentin surfaces were used for the SEM analysis. One piece served as control, and two pieces were treated with 5% MDP ethanol-aqueous solution and ACP-MDP suspension as the above-mentioned. They were dehydrated in a series of

ascending concentrations of ethanol (30-100%) and finally dried with hexamethyldisilazane (HMDS), before they were gold-sputtered and analyzed by an SEM.

2.6.5. TEM analysis

Three 0.5 mm thick resin-bonded dentin slabs (one each group) were obtained during the specimen sectioning for the MTBS tests. The slabs were fixed in Karnovsky's fixative overnight. Subsequently, they were post-fixed in 1% osmium tetroxide. After fixation, they were dehydrated in ascending grades of ethanol (30-100%), and immersed in propylene oxide as a transition fluid. Thereafter, they were embedded in a TEM grade epoxy resin. Finally, non-demineralized ultrathin sections (70-90 nm thick) were prepared with a diamond knife (Diatom, Biel, Switzerland) for TEM analysis.

2.6.6 Statistics

Statistical analysis was performed with the SPSS software package (SPSS Software, version 20.0, IBM SPSS Inc., Chicago, IL, USA). After the data were determined by the Kolmogorov-Smirnov test to follow normal distribution, all the MTBS data were analyzed with one-way ANOVA and LSD analysis. Failure mode data were analyzed using Chi square tests. Statistical significance was preset at $\alpha = 0.05$.

3. Results

Figure 1 reveals the characterization of ACP nanoparticles in the study. TEM (Fig. 1a) and SEM images (Fig. 1b) indicate the diameter of ACP nanoparticles to be approximately 20-100 nm. The FTIR spectrum (Fig. 1c) reveals two typical wide bands. In this study, 0.01 g ACP nanoparticles could released about 0.076 mmol Ca ions.

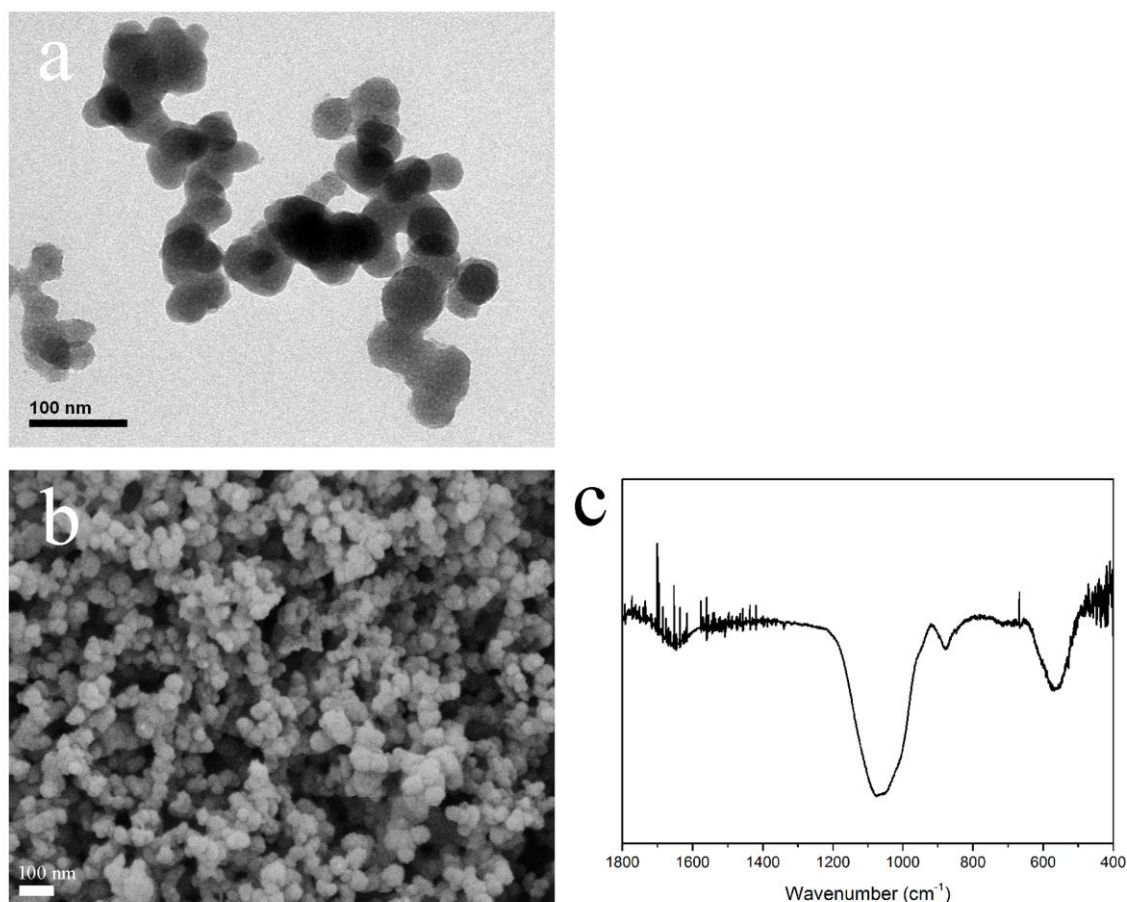


Fig. 1 TEM (a), SEM (b) images and FTIR characterization (c) of the synthetic ACP nanoparticles.

The XRD and TEM findings (Fig. 2) revealed that nano-layering of a highly-ordered structure, ($d=3.88 \pm 0.07$ nm) was initially formed after MDP interacted with ACP nanoparticles for 5 min, and detectable during the experimental period of 5 days. The WAXRD and SAXRD spectrums show three characteristic peaks ($2\theta = 2.26 \pm 0.02^\circ$, $4.59 \pm 0.04^\circ$, $6.80 \pm 0.07^\circ$) and several small peaks ($2\theta = 11.07 \pm 0.03^\circ$, $20.90 \pm 0.11^\circ$, $22.55 \pm 0.09^\circ$) (Figs. 2 a, b). The dark line and light line of the finger-print-like nano-layering structures (Fig. 2c) indicate the MDP-Ca salts and the MDP dimers (Fukeygawa et al., 2006; Ishikawa et al., 1995; Tanaka et al., 1997; Yaguchi et al., 2017; Yaguchi et al., 2017; Yokota et al., 2015), respectively.

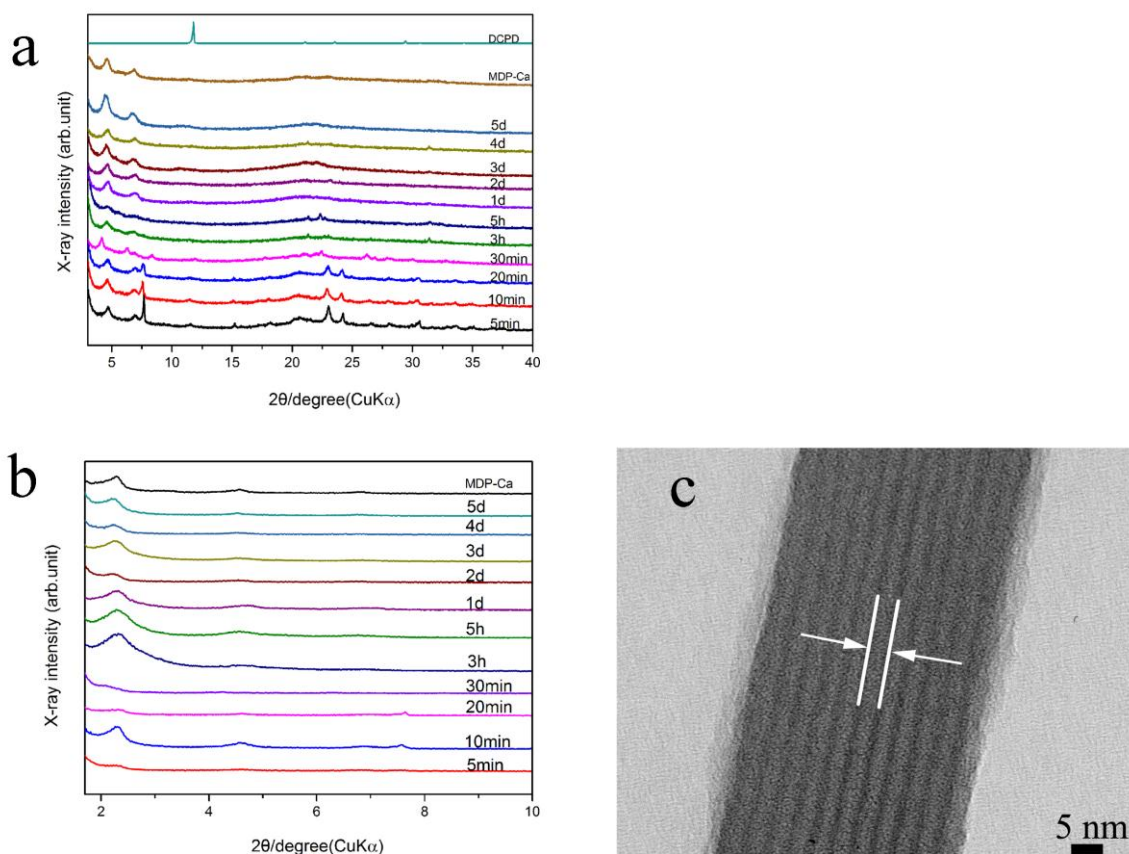


Fig. 2 Wide-(a) and small-angle (b) X-ray diffraction (WAXRD and SAXRD) patterns of the nano-layering after the interaction of MDP solution with ACP nanoparticles from 5 min to 5 d. c: Nano-layering structures were detected by HRTEM after the interaction of MDP solution with ACP nanoparticles. (The dark line: MDP-Ca salts; The light line: the MDP dimers)

The TEM microphotographs (Fig. 3) reveal the direct ultrastructural evidence of the self-assembly process of nano-layering complexes resulting from the interaction of MDP ethanol-aqueous solution with ACP nanoparticles. The nano-layering complexes immediately resulted from the interaction of the ACP nanoparticles with MDP (Fig. 3a). Subsequently, these nanoparticles aggregated as clusters of nanoparticles and coalesce to form beaded structures (Fig. 3b) consisting of the nano-layering structures (Fig. 3c). Afterward, the further interaction between them produced twig-like structures (Fig. 3d) and networks (Fig. 3e). The SEM finding (Fig. 3f) is completely consistent with the TEM microphotographs in this study (Fig. 3 b, d, e).

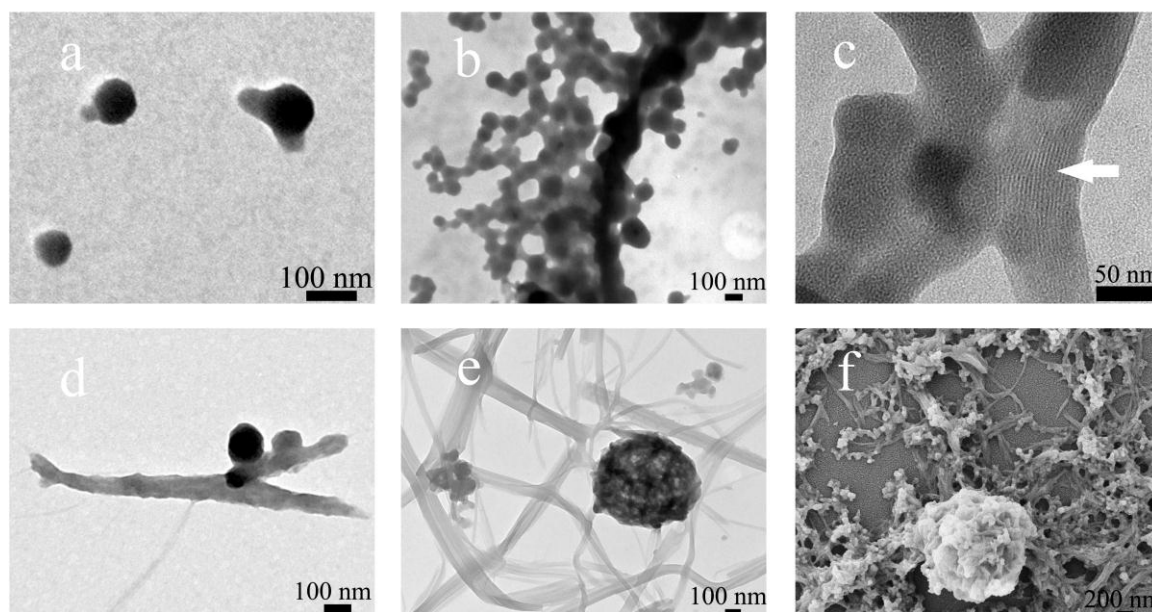


Fig. 3. TEM images (a-e) show the process of the ACP-MDP self-assembly. The shapes of the ACP nanoparticles were changed immediately due to the interaction of ACP and MDP (a). They gradually formed beaded structures (b) composed of nano-layering structures (white arrow) (c). They further formed twig-like structures (d) and the networks (e). The ACP-MDP complex networks on the dentin surface were also confirmed by SEM (f).

However, in the case that either ACP nanoparticles (0.01g) were dispersed in a MDP ethanol-aqueous solution (10% wt, 15% wt or 20% wt), or ACP nanoparticles (0.02 g, 0.03 g or 0.05 g) were dispersed in a 5% wt MDP ethanol-aqueous solution, the nano-layering structure could not be found by TEM and XRD.

HRTEM images (Fig. 4) show that the nano-layering structures were partially degraded by attack with 0.01 mM HCl for 15 min (Fig. 4a), and badly degraded by attack with 5wt% of NaOCl for 15 min (Fig. 4b), but not deteriorated by attack with self-etch adhesive Clearfil S3 Bond for 15 min (Fig. 4c). The nano-layering structures were not changed after 3 months of storage in the ethanol-aqueous suspension (Fig. 4d). AFM force curves (Fig. 4e) reveal that force-deflection line of the rigid silicon substrate was sharp U-turn, while ACP-MDP complexes could resist the load force up to approximately 14 GPa.

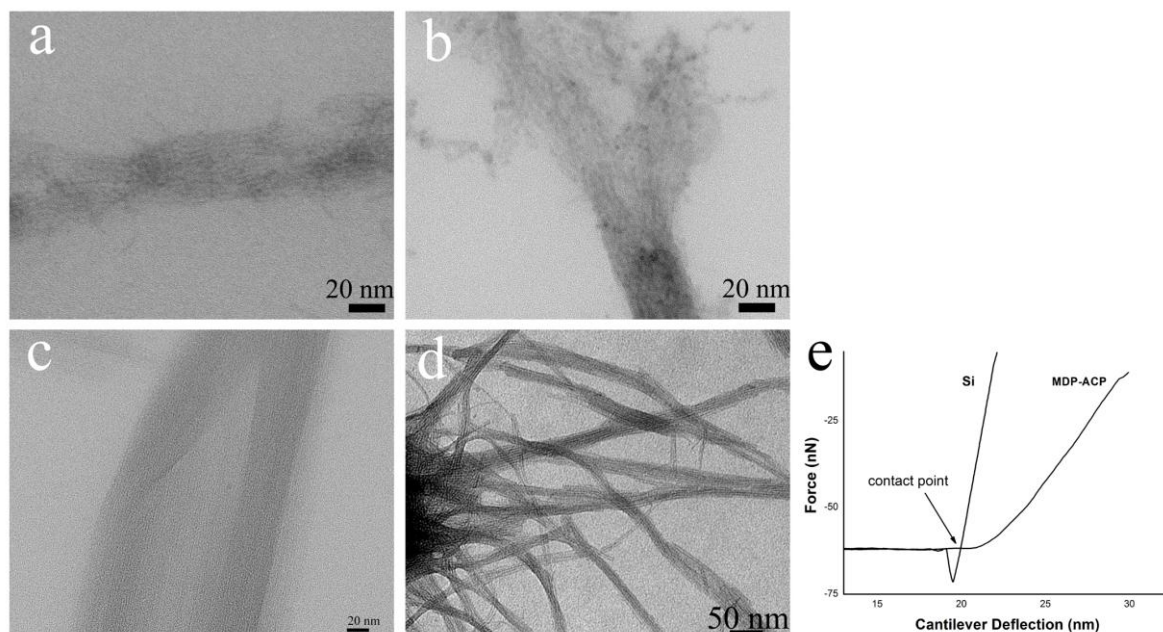


Fig. 4. HRTEM images and AFM force curves The nano-layering structures were partially degraded by challenging with 0.01 mM HCl for 15 mins (a) or badly damaged by challenging with 5wt% of NaOCl for 15 min (b) or not damaged by the self-etch adhesive Clearfil S3 Bond for 15 mins (c). d: The nano-layering structures were stable after 3 months of storage in the ethanol-aqueous ACP-MDP suspension (pH \approx 2.4). e: AFM force curves of silicon substrate and nano-layering structures. Cantilever deflection represents the deformation distance of the sensitive AFM cantilever.

After the dentin surfaces were applied with ACP-MDP suspension or 5% MDP solution, the dentin MTBS could be significantly improved (5% MDP+ACP: 38.92 ± 6.06 Mpa (n=27) ; 5%MDP: 34.44 ± 4.11 Mpa (n=22)), compared with control (24.46 ± 6.11 Mpa (n=25)) ($P < 0.01$). Moreover, the dentin surfaces treated with ACP-MDP suspension produced significantly higher MTBS than those treated with 5% MDP ($P < 0.01$). The frequency distribution of failure modes is graphically presented in Fig. 5. Most of the failure modes were the mixed failure, while there was no significant difference among the three groups ($P > 0.05$).

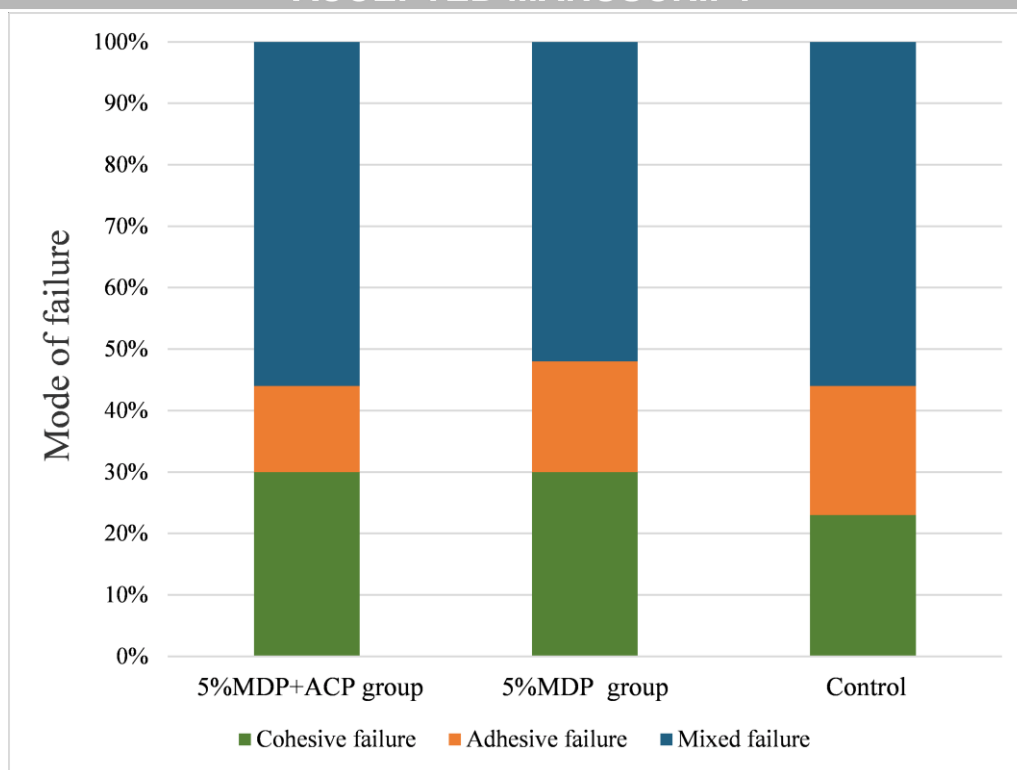


Fig. 5 Failure modes. Mixed failure was predominantly in all three groups.

The SEM findings (Fig. 6a) revealed that the dentin surface was covered by lots of ACP-MDP complexes, after they were treated with ACP-MDP suspension. After pretreatment with 5% MDP, the dentin surfaces were slightly partially demineralized, exposing some fibril-like networks (Fig. 6b). Figure 6c shows that the polishing scratches and polishing debris remained on the dentin surfaces.

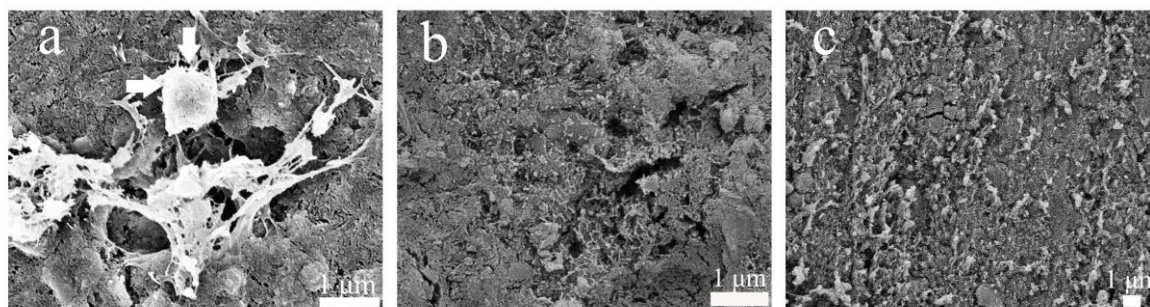


Fig. 6 SEM microphotographs of the differently-treated dentin surfaces. a: After the dentin surface was treated with ACP-MDP suspension, the ACP-MDP complexes (white arrows) were visible on the dentin surfaces. b: After the dentin surface was treated with 5% MDP solution, the dentin surface was slightly partially demineralized, and some fibril-like networks were exposed. c: Control: The polished dentin surface showed some polishing scratch lines.

The TEM microphotographs show that lots of beaded structures of ACP-MDP complexes at the adhesive-dentin interfaces could be detected in the dentin surfaces treated with ACP-MDP suspension (Fig. 7a), but not in the dentin surfaces treated with 5% MDP solution (Fig. 7b) and control (Fig. 7c).

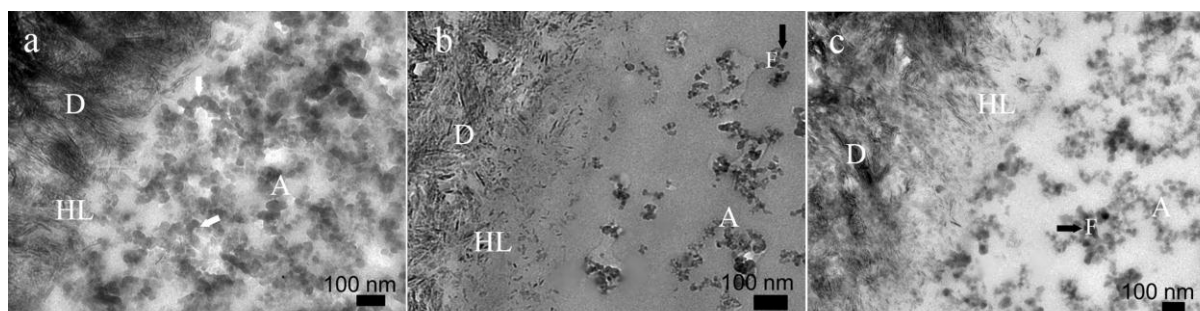


Fig. 7 TEM microphotographs of resin-dentin interface. a: After the dentin surface treated with ACP-MDP suspension, the dentin surface is tightly covered with beaded structures (white arrows) and the dentin was very slightly partially demineralized. Hybrid layer is too thin to be discernible. b: After the dentin surfaces was treated with 5% MDP, lots of short rod-like hydroxyapatite crystallites were visible between a structure-less layer and dentin. c: Control: The partially demineralized dentin was covered with lots of adhesive fillers. D: dentin; HL: hybrid layer; A: adhesive (Clearfil S3 Bond); F: fillers (black arrows).

4. Discussion

The ACP-MDP self-assembly at certain molar ratio of Ca:MDP (0.12:1) went on through a process from ACP nanoparticles, beaded structures, and twig-like structures to networks consisting of nanolayering structures (Fig. 3). However, the process of ACP-MDP self-assembly was not found at the other molar ratios of Ca:MDP. Thus, the null hypothesis that the nano-layering structure could not be self-assembled via a bottom-up way was rejected. The mechanism of the process of ACP-MDP self-assembly has not been clearly elaborated in detail and needs to be further studied.

In this study, the mixture of ACP nanoparticles and the MDP solution at certain ratio could self-assemble into nano-layering with a specific organic-inorganic substructure (Fig. 2). The ACP-MDP nano-layering structure was easily obtained via a simple bottom-up self-assembly at a certain molar ratio. The MDP molecules can chemically absorb onto the surface

of ACP nanoparticles with a strong binding effect between calcium ions and phosphate groups, facilitating the assembly of MDP-Ca salts (Li et al., 2004). MDP molecules can react with calcium ions leaching from ACP nanoparticles due to the attack of hydrogen ion of its own acidic ethanol-aqueous solution ($\text{pH} \approx 2.4$), resulting in a finger-print like structure of periodic nanolayering in this study (Fig. 2c). That is in good agreement with previous research (Fukegawa et al., 2006; Ishikawa et al., 1995; Tanaka et al., 1997; Yaguchi et al., 2017). However, the type of molecular species of MDP-Ca salts could be affected by the molar ratio of calcium ion to MDP (Yokota et al., 2015). In our study, the molar ratio of calcium ion to MDP was 0.12:1. Moreover, the WAXRD and SAXRD spectrums also show a typical three characteristic peaks and several small peaks (Figs. 2 a, b) (Yaguchi et al., 2017; Yokota et al., 2015). That represent mono-calcium salt of the MDP dimer that was predominantly produced in this study, which forms a more tightly-packed nano-layering structure (Yaguchi et al., 2017; Yokota et al., 2015). The periodic nanostructure with a constant interspacing distance (approximately 3.9 nm) was also clearly confirmed by HRTEM (Fig. 2c). In the initial period (5-20 min) of interaction of ACP nanoparticles with the MDP solution, monocalcium phosphate monohydrate (MCPM, $\text{Ca}(\text{H}_2\text{PO}_4)_2 \cdot \text{H}_2\text{O}$) was detected in precipitates by the WAXRD (Fig. 2a), indicating that calcium ions as well as phosphate ions (H_2PO_4^-) were dissolved from ACP nanoparticles. However, MCPM was no longer detected after 20 min of interaction of ACP with MDP, indicating that the initial small amount of MCPM was changed into the other types of calcium phosphate. The insights of this study give a better understanding of the simple ‘bottom-up’ pathway of ACP-MDP assembly and its application.

Structured materials usually possess unique physicochemical properties (Aizenberg et al., 2001; Pokroy et al., 2009). An understanding of controlled formation of biomimetic mesocrystals is essential and important in materials chemistry and engineering (Zhai et al., 2010b). It is worth investigating how two distinct organic and inorganic phases to self-assemble into highly-ordered structures. When the MDP concentrations were increased up to

10 wt%, 15 wt% or 20 wt% in this study, the interaction of ACP nanoparticles (0.01 g) with one of them could not produce the nano-layering structure. In contrary, when the amount of ACP nanoparticles was increased up to 0.02 g, 0.03 g or 0.05 g, the interaction of 5 wt% MDP solution with one of them could not result in nano-layering structures either. In this study, the nano-layering structures were only detected after the interaction of ACP nanoparticles (0.01 g) and 5 wt% of MDP (Figs. 2, 3), indicating that the self-assembly of nano-layering structures occurred at the certain mole ratio of ACP nanoparticles and MDP. Therefore, the cooperative effect of MDP concentrations and amount of ACP nanoparticles was a key factor in the formation of nano-layering structures.

ACP-MDP complexes cannot be subjected to alkaline and acidic challenges (Figs. 4a, 4b), but still stable in the self-etch adhesive (Fig. 4c). ACP-MDP complexes possess similar modulus of elasticity to dentin (Fig. 4e) (Versluis et al., 1996). The findings in this study were supposed that the ACP-MDP complexes remained at the adhesive-dentin interface (Fig. 7a) could greatly increase the dentin MTBS.

To date, MDP-based adhesives have been proven effectively bonding to dentin. (Fujita Nakajima et al., 2018; Teshima et al., 2018; Iwai et al., 2012) The chemisorption of PAEs such as MDP with HAp, enamel and dentin was demonstrated in numerous previous publications (Yoshida et al., 2001; Fu et al., 2005; Fukegawa et al., 2006; Yoshihara et al., 2010; Yoshihara et al., 2011; Zhang, et al., 2013). Chemical bonding at the resin-tooth hard tissue interfaces has been proven to provide a reliable bond (Van Meerbeek et al., 2010). Recently, ACP nanoparticles could be incorporated into self-etch adhesive to deliver the biomimetic mineralization (Wu et al., 2017; Wang et al., 2018).

Prime-and-rinse approach has been reported to improve the enamel bond strengths since the water-soluble calcium salts, which resulted from the demineralization of most enamel smear layer by MDP on the pretreated enamel surfaces, could be washed off (Wang et al., 2013). Prime-and-rinse approach using MDP-containing primer can demineralize dentin

surface and remain some water-insoluble monomer-Ca salts on the dentin surface. However, etch-and-rinse approach using phosphoric acid only demineralizes the dentin surface and cannot produce any water-insoluble monomer-Ca salts. This study is not simple reversal of one-step self-etch adhesives to two-step self-etch adhesives. The novel approach used in this study would not result in the deposits of water-soluble calcium salts along with vaporization, and those water-soluble salts could be rinsed off. In this study, the dentin MTBS could be significantly improved after the dentin surface was treated with prime-and-rinse approach using ACP-MDP suspension. Moreover, the SEM findings (Fig. 6a) revealed that the dentin surfaces treated with ACP-MDP suspension were covered by ACP-MDP complexes. That was supported by the TEM findings that lots of beaded structures at the adhesive-dentin interface (Fig. 3b, 7a).

Furthermore, the dentin surfaces treated with prime-and-rinse approach using ACP-MDP suspension could significantly increase the dentin MTBS when compared with the approach using 5% MDP solution. The dentin MTBS increase might be attributed to the dentin demineralization effect of ACP-MDP suspension as well as chemical bonding of ACP-MDP complexes remained on the dentin surface although the nanolayering structures were not directly detected at the adhesive-dentin interfaces in this study. It is in good agreement with previous research that nano-layering was rarely found in resin-dentin interfaces created by commercial MDP-containing self-etch adhesives (Tian et al., 2016). The ACP-MDP complexes could be endured by challenging with self-etch adhesive for 15 mins (Fig. 4c). Hence, the dentin surfaces could be primed with ACP-MDP suspension prior to application of self-etch adhesive Clearfil S3 Bond. Thus, the null hypothesis that pretreatment with ACP-MDP suspension prior to application of self-etch adhesives could not improve the dentin bond effectiveness was totally rejected. Taken together, these findings imply that the ACP-MDP suspension could be used as a smart material and greatly improve the immediate dentin MTBS before application of self-etch adhesive.

5. Conclusion

According to the limited data in this study, the conclusion could be drawn as follows: The ACP-MDP suspension at certain molar ratio of Ca:MDP (0.12:1) could be self-assembled into ACP-MDP complexes consisting of nanolayering structures. That could be used as a novel primer to greatly improve the dentin MTBS prior to application of self-etch adhesives.

Acknowledgments

This work was supported by the Natural Science Foundation of Zhejiang Province (LQ16H140002, LQ14H140002) and the National Natural Science Foundation of China (81771120).

Declaration of Interest statement

The authors declare no competing financial interests.

References

- Aizenberg, J., Tkachenko, A., Weiner, S., Addadi, L., Hendler, G., 2001. Calcitic microlenses as part of the photoreceptor system in brittlestars. *Nature*. 412, 819-822.
- Armstrong, S., Geraldeli, S., Maia, R., Raposo, L. H., Soares, C. J., Yamagawa, J. 2010. Adhesion to tooth structure: a critical review of "micro" bond strength test methods. *Dent. Mater.* 26, e50-62.
- Breschi, L., Mazzoni, A., Ruggeri, A., Cadenaro, M., Di Lenarda, R., De Stefano Dorigo, E., 2008. Dental adhesion review: aging and stability of the bonded interface. *Dent. Mater.* 24, 90-101.
- Busch, S., Schwarz, U., Kniep, R., 2001. Morphogenesis and Structure of Human Teeth in Relation to Biomimetically Grown Fluorapatite-Gelatine Composites. *Chem. Mater.* 13, 3260-3271.

- Combes, C., Rey, C., 2010. Amorphous calcium phosphates: synthesis, properties and uses in biomaterials. *Acta. Biomater.* 6, 3362-3378.
- Dorozhkin, S. V., Epple, M., 2002. Biological and medical significance of calcium phosphates. *Angew. Chem. Int. Ed.* 41, 3130-3146.
- Fu, B., Sun, X., Qian, W., Shen, Y., Chen, R., Hannig, M., 2005. Evidence of chemical bonding to hydroxyapatite by phosphoric acid esters. *Biomaterials.* 26, 5104-5110.
- Fujita Nakajima, K., Nikaido, T., Francis Burrow, M., Iwasaki, T., Tanimoto, Y., Hirayama, S., Nishiyama, N., 2018. Effect of the demineralisation efficacy of MDP utilized on the bonding performance of MDP-based all-in-one adhesives. *J. Dent.* 77, 59-65.
- Fukegawa, D., Hayakawa, S., Yoshida, Y., Suzuki, K., Osaka, A., Van Meerbeek, B., 2006. Chemical interaction of phosphoric acid ester with hydroxyapatite. *J. Dent. Res.* 85, 941-944.
- Iovan, G., Stoleriu, S., Andrian, S., 2017. Self-etch bonding systems: more reliable or more challenging for the practitioner? *Int. J. Med. Dent.* 21, 189-195.
- Ishikawa, T., Tanaka, H., Yasukawa, A., Kandori, K., 1995. Modification of calcium hydroxyapatite using ethyl phosphonates. *J. Mater. Chem.* 5, 1963-1967.
- Iwai, H., Nishiyama, N., 2012. Effect of calcium salt of functional monomer on bonding performance. *J. Dent. Res.* 91, 1043-1048.
- Jain, S., Udgaonkar, J. B., 2010. Salt-induced modulation of the pathway of amyloid fibril formation by the mouse prion protein. *Biochemistry.* 49, 7615-7624.
- Klement, K., Wieligmann, K., Meinhardt, J., Hortschansky, P., Richter, W., Fändrich, M., 2007. Effect of different salt ions on the propensity of aggregation and on the structure of Alzheimer's $\text{A}\beta(1-40)$ amyloid fibrils. *J. Mol. Biol.* 373, 1321-1333.
- Koshiro, K., Sidhu, S. K., Inoue, S., Ikeda, T., Sano, H., 2006. New concept of resin-dentin interfacial adhesion: the nanointeraction zone. *J. Biomed. Mater. Res. Part. B. Appl. Biomater.* 77, 401-408.

- Li, M., Colfen, H., Mann, S., 2004. Morphological control of BaSO₄ microstructures by double hydrophilic block copolymer mixtures. *J. Mater. Chem.* 14, 2269-2276.
- Liu, Y., Tjäderhane, L., Breschi, L., Mazzoni, A., Li, N., Mao, J., Pashley, D.H., Tay, F.R., 2011. Limitations in bonding to dentin and experimental strategies to prevent bond degradation, *J. Dent. Res.* 90, 953-968.
- Mahamid, J., Sharir, A., Addadi, L., Weiner, S., 2008. Amorphous calcium phosphate is a major component of the forming fin bones of zebrafish: Indications for an amorphous precursor phase. *Proc. Natl. Acad. Sci. U. S. A.* 105, 12748-12753.
- Mann, S., 2001. *Biom mineralization: principles and concepts in bioinorganic materials chemistry.* Oxford University Press, Oxford.
- Manuja, N., Nagpal, R., Pandit, I. K., 2012. Dental adhesion: mechanism, techniques and durability. *J. Clin. Pediatr. Dent.* 36, 223-234.
- Meldrum, F. C., Colfen, H., 2008. Controlling mineral morphologies and structures in biological and synthetic systems. *Chem. Rev.* 108, 4332-4432.
- Niu, L., Zhang, W., Pashley, D., Breschi, L., Mao, J., Chen, J., Tay, F., 2014. Biomimetic remineralization of dentin. *Dent. Mater.* 30, 77-96.
- Pedersen, J. S., Flink, J. M., Dikov, D., Otzen, D. E., 2006. Sulfates dramatically stabilize a salt-dependent type of glucagon fibrils. *Biophys J.* 90, 4181-4194.
- Pokroy, B., Demensky, V., Zolotoyabko, E., 2009. Nacre in Mollusk Shells as a Multilayered Structure with Strain Gradient. *Adv. Funct. Mater.* 19, 1054-1059.
- Tanaka, H., Yasukawa, A., Kandori, K., Ishikawa, T., 1997. Modification of calcium hydroxyapatite using alkyl phosphates. *Langmuir.* 13, 821-826.
- Teshima, M., 2018. Effect of the concentration of water in an MDP-based all-in-one adhesive on the efficacy of smear layer removal and on dentin bonding performance. *Dent. Mater. J.* 37, 685-692.

- Tian, F., Zhou, L., Zhang, Z., Niu, L., Zhang, L., Chen, C., Zhou, J., Yang, H., Wang, X., Fu, B., Huang, C., Pashley, D.H., Tay, F.R., 2016. Paucity of Nanolayering in Resin-Dentin Interfaces of MDP-based Adhesives. *J. Dent. Res.* 95, 380-387.
- Van Landuyt, K. L., Snauwaert, J., De Munck, J., Peumans, M., Yoshida, Y., Poitevin, A., Coutinho, E., Suzuki, K., Lambrechts, P., Van Meerbeek, B., 2007. Systematic review of the chemical composition of contemporary dental adhesives. *Biomaterials.* 28, 3757-3785.
- Van Meerbeek, B., Peumans, M., Poitevin, A., Mine, A., Van Ende, A., Neves, A., De Munck, J., 2010. Relationship between bond-strength tests and clinical outcomes. *Dent. Mater.* 26, e100-e121.
- Versluis, A., Douglas, W. H., Cross, M., Sakaguchi, R. L., 1996. Does an incremental filling technique reduce polymerization shrinkage stresses? *J. Dent. Res.* 75, 871-878.
- Wang, C., Liao, J., Gou, B., Huang, J., Tang, R., Tao, J., Zhang, T., Wang, K., 2009. Crystallization at Multiple Sites inside Particles of Amorphous Calcium Phosphate. *Cryst. Growth. Des.* 9, 2620-2626.
- Wang, X., Wang, C., Zhang, L., Zhang, Z., Fu, B., Hannig, M., 2013. Influence of priming time and primer's concentrations on bovine enamel bond strengths. *J. Adhes. Sci. Technol.* 27, 2558-2570.
- Wang, Z., Ouyang, Y., Wu, Z., Zhang, L., Shao, C., Fan, J., Zhang, L., Shi, Y., Zhou, Z., Pan, H., Tang, R., Fu, B., 2018. A novel fluorescent adhesive-assisted biomimetic mineralization. *Nanoscale.* 10, 18980-18987.
- Weiner, S., Wagner, H. D., 1998. The material bone: Structure mechanical function relations. *Rev. Mater. Sci.* 28,271-298.
- Weiner, S., Sagi, I., Addadi, L., 2005. Structural biology. Choosing the crystallization path less traveled. *Science.* 309, 1027-1028.

- World Medical Association., 2013. World Medical Association Declaration of Helsinki: ethical principles for medical research involving human subjects. *JAMA*. 310, 2191-2194.
- Wu, Z., Wang, X., Wang, Z., Shao, C., Jin, X., Zhang, L., Pan, H., Tang, R., Fu, B., 2017. Self-Etch Adhesive as a Carrier for ACP Nanoprecursors to Deliver Biomimetic Remineralization. *ACS Appl. Mater. Interfaces*. 9, 17710-17717.
- Yaguchi, T., 2017. Layering mechanism of MDP-Ca salt produced in demineralization of enamel and dentin apatite. *Dent. Mater.* 33, 23-32.
- Yokota, Y., Nishiyama, N., 2015. Determination of molecular species of calcium salts of MDP produced through decalcification of enamel and dentin by MDP-based one-step adhesive. *Dent. Mater. J.* 34, 270-279.
- Yoshida, Y., Van Meerbeek, B., Nakayama, Y., Yoshioka, M., Snauwaert, J., Abe, Y., Lambrechts, P., Vanherle, G., Okazaki, M., 2001. Adhesion to and decalcification of hydroxyapatite by carboxylic acids. *J. Dent. Res.* 80, 1565-1569.
- Yoshida, Y., Nagakane, K., Fukuda, R., Nakayama, Y., Okazaki, M., Shintani, H., Inoue, S., Tagawa, Y., Suzuki, K., De Munck, J., Van Meerbeek, B., 2004. Comparative study on adhesive performance of functional monomers. *J. Dent. Res.* 83, 454-458.
- Yoshihara, K., Yoshida, Y., Nagaoka, N., Fukegawa, D., Hayakawa, S., Mine, A., Nakamura, M., Minagi, S., Osaka, A., Suzuki, K., Van Meerbeek, B., 2010. Nano-controlled molecular interaction at adhesive interfaces for hard-tissue reconstruction. *Acta. Biomater.* 6, 3573-3582.
- Yoshihara, K., Yoshida, Y., Hayakawa, S., Nagaoka, N., Irie, M., Ogawa, T., Van Landuyt, K. L., Osaka, A., Suzuki, K., Minagi, S., Van Meerbeek, B., 2011. Nano-layering of phosphoric-acid ester monomer at enamel and dentin. *Acta. Biomater.* 7, 3187-3195.

Zhai, H., Jiang, W., Tao, J., Lin, S., Chu, X., Xu, X., Tang, R., 2010a. Self-Assembled Organic-Inorganic Hybrid Elastic Crystal via Biomimetic Mineralization. *Adv. Mater.* 22, 3729-3734.

Zhai, H., Chu, X., Li, L., Xu, X., Tang, R., 2010b. Controlled formation of calcium-phosphate-based hybrid mesocrystals by organic-inorganic co-assembly. *Nanoscale.* 2, 2456-2462.

Zhang, Z., Wang, X., Zhang, L., Liang, B., Tang, T., Fu, B., Hannig, M., 2013. The contribution of chemical bonding to the short- and long-term enamel bond strengths. *Dent. Mater.* 29, e103-e112.

Accepted manuscript